

# Study of the Hyperon-Nucleon Interaction in Exclusive $\Lambda$ Photo-production off the Deuteron

Nicholas Zachariou<sup>1,2,a</sup>, Yordanka Ilieva<sup>2,b</sup>, and Tongtong Cao<sup>2,c</sup>, for the CLAS Collaboration

<sup>1</sup>University of Edinburgh, Edinburgh, UK

<sup>2</sup>University of South Carolina, Columbia SC, USA

**Abstract.** The study of final-state interactions in exclusive hyperon photoproduction off the deuteron is a promising approach to extract information about the hyperon-nucleon ( $YN$ ) interaction. First preliminary results on the azimuthal asymmetry  $\Sigma$ , as well as the polarization transfer coefficients  $O_x$ ,  $O_z$ ,  $C_x$ , and  $C_z$  for the reaction  $\gamma d \rightarrow K^+ \Lambda n$  initiated with linearly and circularly polarized photon beam are presented. The data were taken with the CLAS detector in Hall B of Jefferson Lab during the E06-103 experiment. The large kinematic coverage of the CLAS, combined with the exceptionally high quality of the experimental data, allows identifying and selecting final-state interaction events to extract single- and double-polarization observables and their kinematical dependencies.

## 1 Introduction

Understanding of the nucleon-nucleon ( $NN$ ) and hyperon-nucleon ( $YN$ ) interaction is necessary in order to obtain a comprehensive picture of the strong interaction. The  $NN$  interaction has been extensively studied for many decades, and a good understanding of this system at energies beyond the pion production threshold exists. On the other hand, direct studies of interactions between other members of the baryon octet remain scarce and inaccurate due to the experimental challenges imposed by short-lived hyperon beams and targets. Reliable data on the  $YN$  interaction will allow for realistic calculations of hypernuclear structure and hyperon matter, and will provide a more detailed understanding of the structure of neutron stars. In addition, the study of the  $YN$  interaction is important for understanding hadron dynamics involving strange quarks, and enables the extension of the baryon-baryon interaction to a more unified picture demanded by  $SU(3)$  symmetry.

$YN$  potentials, constructed from  $NN$  potentials under the assumption of exact  $SU(3)$  symmetry, have several free parameters that must be constrained from experimental data. The best approach to constrain these is to use  $YN$  elastic scattering, but the challenges imposed by hyperon beams and targets result in data of poor quality and energy limitations. This has prompted interest in complimentary studies that allow indirect access to the dynamics of the  $YN$  interaction through hypernuclear studies and studies of final state interactions (FSI). Our work utilises the sufficient counting rates that are obtained with the use of modern accelerators to study FSI in exclusive hyperon photoproduction off a

---

<sup>a</sup>e-mail: [nicholas@jlab.org](mailto:nicholas@jlab.org)

<sup>b</sup>e-mail: [ilieva@sc.edu](mailto:ilieva@sc.edu)

<sup>c</sup>e-mail: [caot@email.sc.edu](mailto:caot@email.sc.edu)

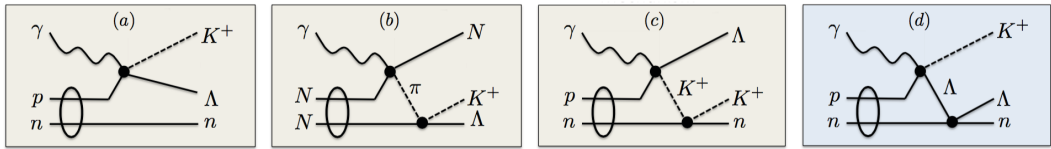


**Figure 1.** Four main mechanisms that contribute to the reaction  $\gamma d \rightarrow K^+ \Lambda n$  according to theoretical models [1, 2]: (a) quasi-free  $\Lambda$  photoproduction on the proton; (b) pion mediated production; (c)  $K^+$  rescattering on spectator neutron; (d)  $\Lambda$  rescattering on spectator neutron.

deuterium target. The simplicity of the target, as well as the fact that the electromagnetic interaction is well understood, allows us to select kinematics where FSI between the hyperon and the spectator nucleon are greatly enhanced.

According to the available models [1, 2], several mechanisms contribute to the reaction  $\gamma d \rightarrow K^+ \Lambda n$ ; the main ones are shown in Fig. 1. The exclusivity of the reaction allows us to select kinematics that minimize contributions from the quasi-free (QF) mechanism, which dominates the cross section. This enhances contributions from FSI, giving us the ability to extract information of the dynamics of  $YN$  in a model-dependent way. Currently, the most comprehensive model for this reaction allows calculations of the unpolarized differential cross section, as well as single- and double- polarization observables [1, 3]. This model makes predictions using two  $YN$  potentials (Nijmegen NSC89 and NSC97f), both of which correctly predict the hypertriton binding energy [4] and take into account contributions from the QF reaction. The predictions clearly indicate sensitivities of polarization observables to the  $YN$  potentials at certain kinematics. A large sample of polarization observables is expected to place stringent constraints on the theoretical models and allow us to extract information of the dynamics of the  $YN$  interaction.

In addition, a new theoretical approach allows the extraction of the spin-averaged  $\Lambda - n$  scattering lengths by studying the  $\Lambda - n$  invariant mass distributions of observables [5]. This approach has been tested on inclusive  $K^+$  hadron-production data and on pseudodata on deuteron photoproduction indicating that the current poorly-determined scattering lengths can be further constrained from FSI.

## 2 Experimental Procedure

Polarization observables for FSI in the reaction  $\gamma d \rightarrow K^+ \Lambda n$  were determined using data collected with the CEBAF Large Acceptance Spectrometer (CLAS) [6] housed in Hall B of Jefferson Lab in Newport News, Virginia. The experiment E06-103 utilised both linearly- and circularly-polarized photon beams and took place in 2006 and 2007 [7]. Photons with average linear polarization of 75%, produced via coherent bremsstrahlung, gave access to  $\Sigma$ ,  $O_x$ , and  $O_z$ . Photons produced using a thin gold radiator with circular polarizations between 30% and 80% gave access to  $C_x$  and  $C_z$ . Three charged-track events were selected identifying the  $K^+$  and the  $p\pi^-$  pair from the  $\Lambda$  decay. The hyperon was reconstructed from the  $p\pi^-$  invariant mass and the reaction was identified using the missing-mass technique. The upper panel of Fig. 2 shows the missing mass of the reaction  $\gamma d \rightarrow K^+ \Lambda X$ , in which one can clearly identify missing-neutron events over a smooth background from  $\Sigma^0$  and  $\Sigma^*$  photoproduction events. Background contributions were studied in detail utilizing a comprehensive event generator (developed by the authors) and a realistic detector simulation [8] and subtracted from the total yield to obtain a clean signal.

Contributions from the QF mechanism were significantly reduced by selecting events in which the final neutron had momentum higher than the typical Fermi momentum. The neutron momentum

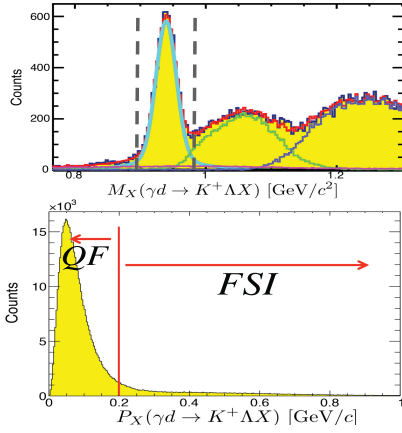


**Figure 2.** Top panel: Missing-mass distribution of the reaction  $\gamma d \rightarrow K^+ \Lambda X$  fitted with contributions from  $\gamma d \rightarrow K^+ \Sigma^0 X$  (green),  $\gamma d \rightarrow K^+ \Sigma^+ X$  (purple), and accidental events (magenta) from simulated data. The vertical dotted lines indicate the cuts that select the events of interest and the fits are used to perform background subtraction. Bottom panel: Missing momentum of the reaction  $\gamma d \rightarrow K^+ \Lambda X$  indicating the cut applied to select FSI.

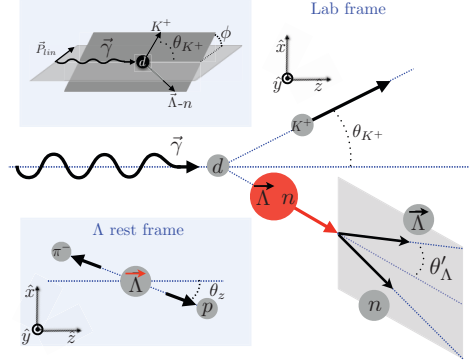


**Figure 3.** Reaction plane definition for  $\gamma d \rightarrow K^+ \Lambda n$ . The upper left panel shows the definition of the kaon azimuthal angle  $\phi$  in which  $\Sigma$  produces a modulation (see Eq. [1]). The lower left panel shows the definition of  $\theta_z$  (and correspondingly  $\theta_x$ ) in which the double-polarization observables produce modulations. The main figure defines the kaon laboratory polar angle  $\theta_{K^+}$ , and the hyperon angle  $\theta'_\Lambda$ , which is in respect to an axis pointing along the momentum of the  $YN$  pair.

was reconstructed through four-momentum conservation, with the cut to select FSI indicated on the bottom panel of Fig. 2.

The polarization observables were determined using a maximum likelihood technique. A multi-dimensional minimization was performed on each of the linearly and circularly polarized data, and from this, each set of polarization observables were determined. The likelihood function was modelled according to the polarized cross section

$$\frac{d\sigma}{d\Omega} = \frac{d\sigma}{d\Omega}_0 \left[ 1 - P_{lin} \Sigma \cos 2\phi + \alpha \cos \theta_x (-P_{lin} O_x \sin 2\phi - P_{circ} C_x) - \alpha \cos \theta_y (-P_y + P_{lin} T \cos 2\phi) - \alpha \cos \theta_z (P_{lin} O_z \sin 2\phi + P_{circ} C_z) \right], \quad (1)$$

where  $\frac{d\sigma}{d\Omega}_0$  is the unpolarized cross section,  $P_{lin}$  and  $P_{circ}$  are the degree of linear and circular polarization, respectively, and  $\Sigma$ ,  $O_x$ ,  $O_z$ ,  $C_x$ ,  $C_z$ ,  $P_y$ , and  $T$  are the polarization observables. The angles  $\phi$ , and  $\theta_{x,y,z}$  are defined in Fig 3. The self-analyzing power of  $\Lambda$ , which allows the determination of the  $\Lambda$  polarization by studying the distribution of its decay products, is denoted by  $\alpha$ .

### 3 Results and Discussion

Preliminary results for polarization observables of FSI in the reaction  $\gamma d \rightarrow K^+ \Lambda n$  were determined. Specifically,  $\Sigma$ ,  $O_x$ ,  $O_z$ ,  $C_x$ , and  $C_z$  were determined for photon energies between 1.0 and 2.4 GeV, kaon momenta between 0.3 and 1.9 GeV/c, and  $\theta'_\Lambda$  angles between 0 and 60 degrees as shown in Fig. 4. Invaluable information on kinematic regions where specific FSI are enhanced can be extracted from studying the differences between the observables determined for the QF reaction and FSI (see Fig. 4).

Our preliminary results clearly indicate that the data are of sufficient statistics to study kinematical dependencies of several polarization observables with adequate precision. Three-fold and four-fold differential results can also be extracted with acceptable statistical uncertainties. These are very important due to their larger sensitivity to details of the theoretical models. Such results were extracted for  $\Sigma$ ,  $C_x$ , and  $C_z$  and a detailed study of these in collaboration with theorists is underway. The  $\Lambda - n$

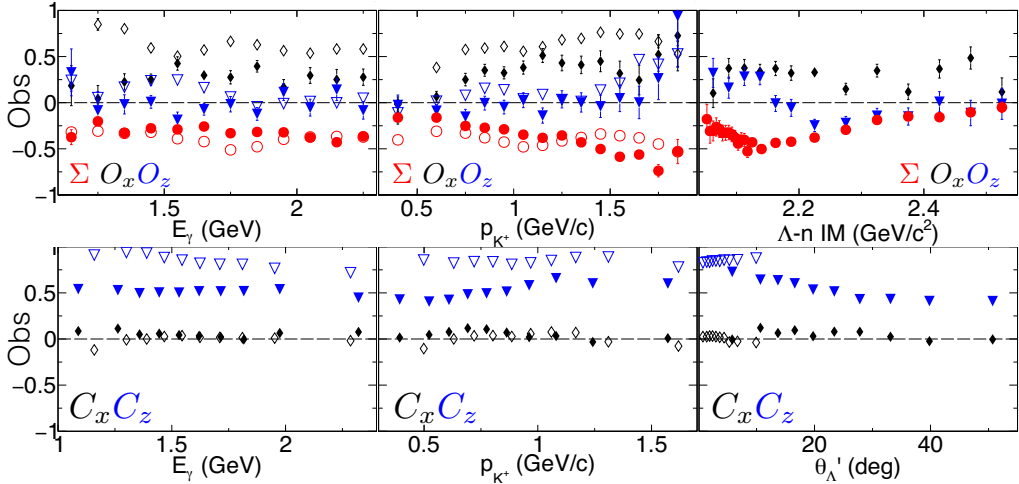


**Figure 4.** First preliminary results for FSI (solid markers) and QF (open markers) in the reaction  $\gamma d \rightarrow K^+ \Lambda n$ . The top row indicates polarization observables determined from data collected from the linearly polarized photon beam and the bottom row from the circularly polarized photon beam. The dependences of the observables on the incident photon energy ( $E_\gamma$ ), kaon momentum ( $p_{K^+}$ ),  $\Lambda - n$  invariant mass, and the angle of  $\Lambda$  ( $\theta'_\Lambda$ ) are shown.

invariant mass dependence of these observables was also determined (see Fig. 4 upper right panel). These results will be used to extract the spin-averaged  $\Lambda - n$  scattering length using the approach in Ref. [5]. It is expected that the result from this work will provide a scattering length that is better constrained than the one obtained from elastic scattering data.

Extraction of additional polarization observables, such as  $P_y$ ,  $T$ , and especially beam-spin asymmetries defined using the azimuthal distribution of the  $\Lambda$  or the  $\Lambda - n$  pair will give additional information on FSI and may allow us to identify kinematics where specific rescattering mechanism dominates. Our set of observables will be fitted to theoretical models in order to constrain the free parameters of YN potentials.

## References

- [1] A. Salam *et al.*, Phys. Rev. C **74**, 044004 (2006)
- [2] J. M. Laget, Phys. Rev. C **75**, 014002 (2007)
- [3] K. Miyagawa *et al.*, Phys. Rev. C **74**, 034002 (2006);
- [4] K. Miyagawa *et al.*, Nucl. Phys. **A639**, 297c (1998)
- [5] A. Gasparian *et al.*, Phys. Rev. C **69**, 034006 (2004)
- [6] B. A. Mecking *et al.*, Nucl. Instr. and Meth. A **503**, 513 (2003)
- [7] P. Nadel-Turonski *et al.*, Jefferson Lab PAC30 Proposal PR-06-103 (2006)
- [8] E. Wolin, *GSIM Documentation*, <http://www.jlab.org/Hall-B/document/gsim/userguide.html>